ISSN 1067-8212, Russian Journal of Non-Ferrous Metals, 2018, Vol. 59, No. 6, pp. 637–642. © Allerton Press, Inc., 2018.
Original Russian Text © A.Yu. Churyumov, V.V. Spasenko, D.M. Hazhina, A.V. Mikhaylovskaya, A.N. Solonin, A.S. Prosviryakov, 2018, published in Izvestiya Vysshikh Uchebnykh Zavedenii, Tsvetnaya Metallurgiya, 2018, No. 5, pp. 66–71.

PHYSICAL METALLURGY AND HEAT TREATMENT

Study of the Structural Evolution of a Two-Phase Titanium Alloy during Thermodeformation Treatment

A. Yu. Churyumov[a], *, V. V. Spasenko[a], D. M. Hazhina[a], A. V. Mikhaylovskaya[a], **, A. N. Solonin[a], *, and A. S. Prosviryakov[a], ******

[a] *National University of Science and Technology "MISiS", Moscow, 119049 Russia*

**e-mail: churyumov@misis.ru*

***e-mail: mihaylovskaya@misis.ru*

****e-mail: solonin@misis.ru*

*****e-mail: pro.alex@mail.ru*

Received December 12, 2017; in final form, April 23, 2018; accepted for publication April 27, 2018

Abstract—The behavior of the Ti–3.5Fe–4Cu–0.2B two-phase titanium alloy during thermal-deformation treatment under uniaxial compression is investigated. Boron is introduced to form a fine-grained structure in a cast state. Alloy samples 6 mm in diameter are formed by alloying pure components in a vacuum induction furnace and subsequent accelerated crystallization in a massive copper mold. The tests for uniaxial compression with true deformation of 0.9 are performed using a Gleeble 3800 physical simulation system of thermomechanical processes at 750, 800, and 900°C and strain rates of 0.1, 1, and 10 s^{-1}. The alloy microstructure in the initial and deformed states is investigated using scanning electron microscopy. The tests result in a model of the dependence of the flow stress on temperature and strain rate. It is shown that the recrystallization of the initial cast structure containing solid solutions based on α-Ti, β-Ti, and titanium diboride colonies occurs during pressure treatment. The volume fraction of the solid solution grains based on α-titanium decreases during deformation with an increase in temperature, while the fraction of the β phase, on the contrary, increases. Herewith, the average grain size of solid solutions based on α-Ti and β-Ti varies insignificantly after deformation according to almost all studied modes. It is shown that the preferential mode of the pressure heat treatment for attaining the high complex of mechanical properties in the alloy under study is a temperature range of 750–800°C because the grain size of the α phase increases from 2.2 to 4.5 μm with an increase in temperature up to 900°C.

Keywords: two-phase titanium alloy, rheological model, microstructure

DOI: 10.3103/S1067821218060032

INTRODUCTION

Modern industry has increasingly rigorous demands for the structure and mechanical properties of construction and functional materials. Titanium alloys possess a unique combination of corrosion resistance and strength at room and elevated temperatures having sufficiently low density [1–12]. Due to their properties, titanium alloys have found broad application in aerospace, transport, and chemical industry, as well as in biomedicine. Two-phase titanium alloys of a martensite class are widely used, and all types of semifinished products are fabricated from them. However, one substantial disadvantage of these alloys is a considerable amount of alloying elements entering the composition, including high-cost ones: up to 6.9 Al, 4.5 V, and 5.0 Mo. The authors of [13–17] previously showed that codoping with iron and copper positively affects the structure of forged titanium alloys. However, in connection with the insufficient manufacturability of these alloys, the investigation into the deformation behavior and microstructure evolution in a broad range of strain rates and temperatures, as well as the construction of the rheological model of the relation of the flow stress with the plastic deformation parameters, are required to accelerate the development of industrial methods of pressure treatment. The goal of this study is to determine the deformation stress under compression and study the influence of thermal-deformation treatment modes on the structure of the Ti–3.8Fe–4.4Cu–0.2B titanium alloy.

EXPERIMENTAL

We selected the Ti–3.8Fe–4.4Cu–0.2B alloy[1] as the object of investigation. Boron was introduced to fabricate the fine-grained structure in a cast state.

[1] Here and below, wt %.

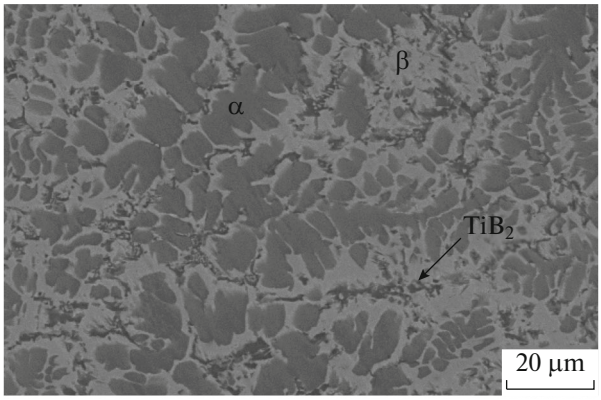

Fig. 1. Microstructure of the Ti–3.8Fe–4.4Cu–0.2B alloy in the cast state.

Alloy ingots 6 mm in diameter were fabricated by alloying pure components in a vacuum induction furnace and subsequent accelerated crystallization into a massive copper mold under an argon pressure of 0.3 MPa. We found three ingots of one composition 6 × 50 mm in size, of which the samples 10 mm in height were cut.

The uniaxial compression tests with true strain $\varepsilon = 0.9$ were performed using a Gleeble 3800 physical simulation system of thermomechanical processes (DSI, United States) at 750, 800, and 900°C and strain rates of 0.1, 1, and 10 s^{-1}. A cylindrical sample cut from an ingot 6 mm in diameter and 10 mm in height was clamped into tungsten carbide heads, heated to the testing temperature with a rate of 5 K/s by direct current flowing, and held for 10 s. The sample temperature was monitored using a chromel–alumel thermocouple soldered to a central sample part. Graphite foil and a nickel-based lubricant were laid between the heads and sample faces to decrease friction during the test. Heating and deformation were performed under high vacuum (the residual pressure was smaller than 10^{-3} Pa). After the test, the sample was forcedly cooled by a compressed air jet for further microstructural analysis. The measured cooling rate in a temperature range of 900–500°C was larger than 50 K/s, which is higher than the critical rate for most titanium alloys.

In order to determine the true stress, we corrected the primary data according to the procedure [18]. This correction is necessary because of the temperature variation during the deformation (which is especially important for tests with increased rates) and also because of the presence of friction between the heads and a sample.

The alloy microstructure in the initial and deformed states was investigated by scanning electron microscopy (SEM) using a Tescan Vega 3 LMH microscope with an X-Max 80 energy dispersion detector (Tescan, Czech Republic). The chemical composition of alloys was determined by electron probe microanalysis of five microstructure segments 100 × 100 μm in size. Slices for microstructural investigations were prepared using a Struers LaboPol-5 grinding–polishing machine (Struers, Netherlands).

RESULTS AND DISCUSSIONS

The structure of the Ti–3.8Fe–4.4Cu–0.2B alloy in the cast state (Fig. 1) consists of α phase (dark segments), β phase (light segments), and titanium boride TiB_2 (dark particles). The results of an analysis of the chemical composition and volume fraction of phases are presented in Table 1. It is seen that the larger part of iron and copper dissolved in the bcc lattice of β-Ti, while only a small amount of copper is dissolved in α-Ti with the hcp lattice.

Compression curves of the samples are presented in Fig. 2. It is seen that the flow stress regularly increases with an increase in the rate and a decrease in temperature. A maximum is observed at the initial compression stage at all temperatures and strain rates, after which the flow stress decreases, which is caused by the active development of dynamic recrystallization.

Table 1. Volume fraction, average chemical composition, and average phase size in the cast state

Phase	Fraction, vol %	Average grain size, μm	Content, wt %			
			Fe	Cu	B	Ti
Average composition*						
	–	–	3.8 ± 0.3	4.4 ± 0.2	–	Res.
α phase	59 ± 1	2.5 ± 0.2	–	0.7 ± 0.3	–	Res.
β phase	38 ± 1	1.7 ± 0.2	7.1 ± 0.2	7.7 ± 0.4	–	Res.
TiB_2 borides	3.0 ± 0.5	1.1 ± 0.2	–	–	12.7 ± 0.7	Res.

*Average chemical composition by the results of 15 measurements is presented.

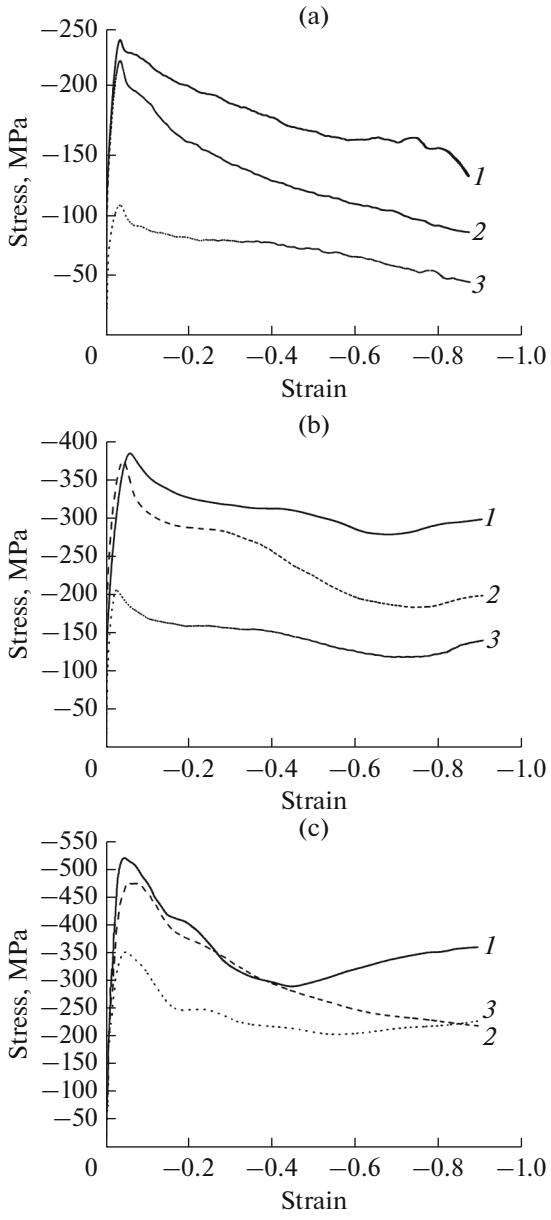

Fig. 2. Deformation curves at a rate of (a) 0.1, (b) 1, and (c) 10 s^{-1}. *t*, °C: (*1*) 750, (*2*) 800, and (*3*) 900.

The relation between the flow stress at the stated stage, rate, and deformation temperature is described well by the Arrhenius equation [19]:

$$\dot{\varepsilon} = A\sigma^n e^{-\frac{Q}{RT}}, \quad (1)$$

where $\dot{\varepsilon}$ is the deformation rate, s^{-1}; T is the temperature, K; Q is the effective deformation energy, J/mol; and A, n are constants.

Unknown parameters A, n, and Q were found by minimizing the error between calculated and experimental values of the flow stress at the degree of deformation of 0.5 corresponding to the stated deformation stage. This results in $A = 7.4$, $n = 4.1$, and $Q = 220$ kJ/mol. An average calculation error according to the designed model was 6%. The effective activation energy of deformation lies between the activation energy of self-diffusion in α-titanium (it is from 169.1 [20] to 193 kJ/mol [21]) and in β-titanium (251.2 [20] and 282.9 kJ/mol [22]), which evidences that both phases actively participate in the deformation process. Our values of model parameters can be used when constructing finite-element models and optimizing the technology of actual pressure-treatment processes.

It follows from Fig. 3 that the structure of the samples quenched from the deformation temperature is presented by α and β phases and boride inclusions. It is seen that inclusions of titanium borides during the

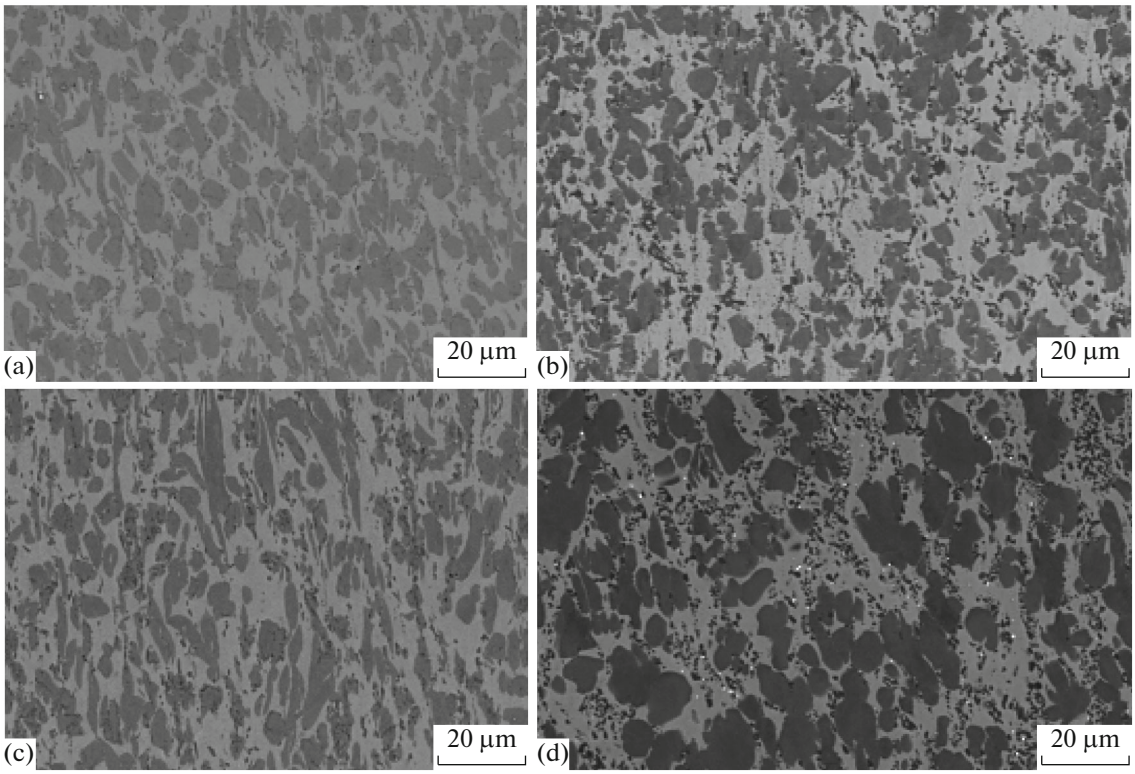

Fig. 3. Microstructure of the samples in the deformed state. (a) $\dot{\varepsilon} = 0.1\ s^{-1}$, $t = 750°C$; (b) $\dot{\varepsilon} = 0.1\ s^{-1}$, $t = 900°C$; (c) $\dot{\varepsilon} = 10\ s^{-1}$, $t = 750°C$; and (d) $\dot{\varepsilon} = 10\ s^{-1}$, $t = 900°C$.

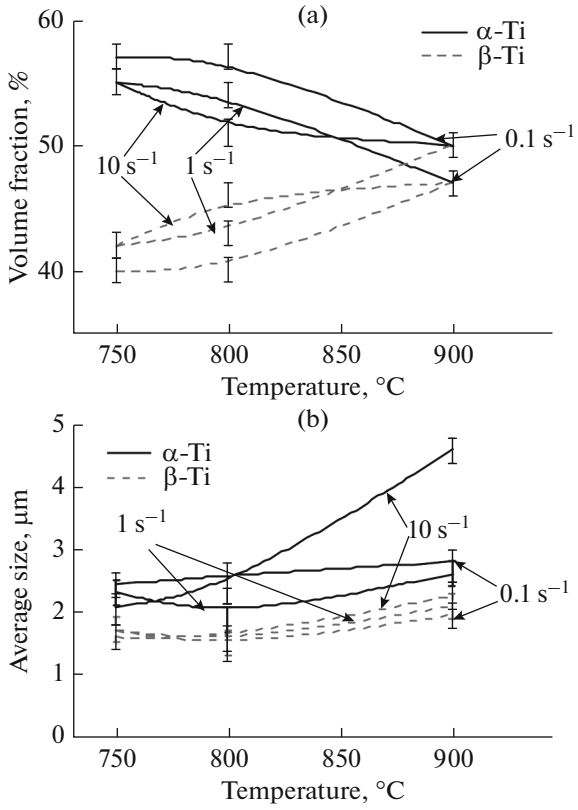

Fig. 4. Dependence of the (a) volume fraction and (b) grain size of α and β phases on temperature and strain rate of the Ti–3.8Fe–4.4Cu–0.2B alloy.

deformation divide into separate particles 0.5–1.5 μm in size distributed with higher uniformity than in the cast state. Herewith, the average grain size of α and β phases varies insignificantly after deformation according to almost all studied modes. The grain growth of the α phase is found only during deformation according to the mode $t = 900°C$ and $\dot{\varepsilon} = 10\ s^{-1}$ (Figs. 3d, 4b). This can be associated with adiabatic sample heating at a high strain rate. In addition, the dynamic recrystallization and globularization of the α phase possibly occur at $t = 900°C$ and $\dot{\varepsilon} = 0.1\ s^{-1}$ [23], while these processes have no time to proceed completely at $\dot{\varepsilon} = 10\ s^{-1}$. The recrystallization and grain growth in the heavier alloyed β phase can be retarded by the atoms of alloying components, which is why the grain size of the β phase does not vary considerably. The volume ratio between α and β phases decreases with an increase in the deformation temperature irrespective of the rate (Fig. 4a).

CONCLUSIONS

(i) The microstructure of the Ti–3.8Fe–4.4Cu–0.2B alloy in the cast state and after hot deformation under uniaxial compression in various temperature-rate conditions is investigated. The alloy structure in the cast and deformed states contains α phase, β phase, and titanium diboride particles. It is shown that the β phase contains up to 7.1% Fe and 7.7% Cu in the cast state and is considerably more heavily alloyed when compared the α phase containing 0.7% Cu.

(ii) Compression tests of the Ti–3.8Fe–4.4Cu–0.2B alloy are performed at 750–900°C and deformation rates 0.1–10 s^{-1}, and a model of relation of the flow stress with thermal-deformation treatment parameters is designed.

(iii) It is shown that the preferential hot-treatment pressure mode for the formation of the fine-grained structure in the studied alloy is a temperature range of 750–800°C because the grain size of the α phase increases from 2.2 to 4.5 μm with an increase in temperature to 900°C. The studied alloy has prospects of using as economically alloyed material of an increased corrosion resistance and strength.

ACKNOWLEDGMENTS

This study was supported by the Ministry of Education and Science of the Russian Federation in the scope of state tasks to higher schools for 2017–2020, project no. 11.7172.2017/8.9.

REFERENCES

1. Il'in, A.A., Kolachev, B.A., and Pol'kin I.S., *Titanovye splavy. Sostav, struktura, svoistva* (Titanium Alloys. Composition, Structure, Properties), Moscow: VILS–MATI, 2009.
2. Cui, C., Hu, B., Zhao, L., and Liu, S., Titanium alloy production technology, market prospects and industry development, *Mater. Design.*, 2011, vol. 32, no. 3, pp. 1684–1691. https://doi.org/10.1016/j.matdes.2010.09.011.
3. Hayama, A.O.F., Lopes, J.F.S.C., da Silva, M.J.G., Abreu, H.F.G., and Caram, R., Crystallographic texture evolution in Ti–35Nb alloy deformed by cold rolling, *Mater. Design.*, 2014, vol. 60, pp. 653–660. https://doi.org/10.1016/j.matdes.2014.04.024.
4. Li, C., Chen, J. H., Wu, X., and Zwaag, S., A comparative study of the microstructure and mechanical properties of α + β titanium alloys, *Met. Sci. Heat Treat.*, 2014, vol. 56, nos. 7–8, pp. 374–380. https://doi.org/10.1007/s11041-014-9765-2.
5. Lu, J., Ge, P., Li, Q., Zhang, W., Huo, W., Hu, J., Zhang, Y., and Zhao, Y., Effect of microstructure characteristic on mechanical properties and corrosion behavior of new high strength Ti-1300 beta titanium alloy, *J. Alloys Compd.*, 2017, vol. 727, pp. 1126–1135. https://doi.org/10.1016/j.jallcom.2017.08.239.
6. Li, Y.-H., Chen, N., Cui, H.-T., and Wang, F., Fabrication and characterization of porous Ti–10Cu alloy for biomedical application, *J. Alloys Compd.*, 2017, vol. 723, pp. 967–973. https://doi.org/10.1016/j.jallcom.2017.06.321.
7. Shi, X., Zeng, W., Long, Y., and Zhu, Y., Microstructure evolution and mechanical properties of near-α Ti–8Al–1Mo–1V alloy at different solution temperatures and cooling, *J. Alloys Compd.*, 2017, vol. 727, pp. 555–564. https://doi.org/10.1016/j.jallcom.2017.08.165.
8. Chuvil'deev, V.N., Kopylov, V.I., Nokhrin, A.V., Tryaev, P.V., Kozlova, N.A., Tabachkova, N.Yu., Lopatin, Yu.G., Ershova, A.V., Mikhaylov, A.S., Gryaznov, M.Yu., and Chegurov, M.K., Study of mechanical properties and corrosive resistance of ultrafine-grained α-titanium alloy Ti–5Al–2V, *J. Alloys Compd.*, 2017, vol. 723, pp. 354–367. https://doi.org/10.1016/j.jallcom.2017.06.220.
9. Zhao, G.-H., Ketov, S.V., Jiang, J., Mao, H., Borgenstam, A., and Louzguine-Luzgin, D.V., New beta-type Ti–Fe–Sn–Nb alloys with superior mechanical strength, *Mater. Sci. Eng. A*, 2017, vol. 705, pp. 348–351. https://doi.org/10.1016/j.msea.2017.08.060.
10. Nochovnaya, N.A., Khorev, A.I., and Yakovlev, A.L., Perspectives of alloying titanium alloys with rare earth elements, *Met. Sci. Heat Treat.*, 2013, vol. 55, nos. 7–8, pp. 415–418. https://doi.org/10.1007/s11041-013-9646-0.
11. Popov, A.A., Leder, M.O., Popova, M.A., Rossina, N.G., and Narygina, I.V., Effect of alloying on precipitation of intermetallic phases in heat-resistant titanium alloys, *Phys. Met. Metallogr.*, 2015, vol. 116, no. 3, pp. 261–266. https://doi.org/10.1134/S0031918X15030102.
12. Gaisin, R.A., Imayev, V.M., Imayev, R.M., and Gaisina, E.R., Microstructure and hot deformation behavior of two-phase boron-modified titanium alloy VT8, *Phys. Met. Metallogr.*, 2013, vol. 114, no. 4, pp. 339–347. https://doi.org/10.1134/S0031918X13040042.
13. Zadorozhnyy, V.Yu., Shchetinin, I.V., Zheleznyi, M.V., Chirikov, N.V., Wada, T., Kat, H., and Louzguine-

Luzgin, D.V., Investigation of structure–mechanical properties relations of dual-axially forged Ti-based low-alloys, *Mater. Sci. Eng. A*, 2015, vol. 632, pp. 88–95. https://doi.org/10.1016/j.msea.2015.02.065.

14. Zadorozhnyy, V.Yu., Inoue, A., and Louzguine-Luzgin, D.V., Investigation of the structure and mechanical properties of as-cast Ti–Cu-based alloys, *Mater. Sci. Eng. A*, 2013, vol. 573, pp. 175–182. https://doi.org/10.1016/j.msea.2013.02.031.
15. Zadorozhnyy, V.Yu., Kozak, D.S., Shi, X., Wada, T., Louzguine-Luzgin, D.V., and Kato, H., Mechanical properties, electrochemical behavior and biocompatibility of the Ti-based low-alloys containing a minor fraction of noble metals, *J. Alloys Compd.*, 2018, vol. 732, pp. 915–921. https://doi.org/10.1016/j.jallcom.2017.10.231.
16. Zadorozhnyy, V.Yu., Shchetinin, I.V., Chirikov, N.V., and Louzguine-Luzgin, D.V., Tensile properties of a dual-axial forged Ti–Fe–Cu alloy containing boron, *Mater. Sci. Eng. A*, 2014, vol. 614, pp. 238–242. https://doi.org/10.1016/j.msea.2014.07.017.
17. Zadorozhnyy, V.Yu., Inoue, A., and Louzguine-Luzgin, D.V., Ti-based nanostructured low-alloy with high strength and ductility, *Mater. Sci. Eng. A*, 2012, vol. 551, pp. 82–86. https://doi.org/10.1016/j.msea.2012.04.097.
18. Churyumov, A.Yu., Khomutov, M.G., Tsar'kov, A.A., Pozdnyakov, A.V., Solonin, A.N., Efimov, V.M., and Mukhanov, E.L., Study of the structure and mechanical properties of corrosion-resistant steel with a high concentration of boron at elevated temperatures, *Phys. Met. Metallogr.*, 2014, vol. 115, pp. 809–813. https://doi.org/10.1134/S0031918X14080031.
19. Sellars, C.M. and McTegart, W.J., On the mechanism of hot deformation, *Acta Metall.*, 1966, vol. 14, pp. 1136–1138. https://doi.org/10.1016/0001-6160(66)90207-0.
20. Gale, W.F. and Totemeier, T.C., *Smithells Metals Reference Book*, Oxford: Butterworth-Heinemann, 2004, 8th ed.
21. Perez, R.A., Nakajima, H., and Dyment, F., Diffusion in α-Ti and Zr, *Mater. Trans., J*2003, vol. 44, no. 1, pp. 2–13. https://doi.org/10.2320/matertrans.44.2.
22. Neumann, G. and Tuijn, C., *Self-Diffusion and Impurity Diffusion in Pure Metals: Handbook*, Amsterdam: Elsevier, 2009.
23. *Titanovye splavy. Metallografiya titanovykh splavov* (Titanium Alloys. Metallography of Titanium Alloys), Anoshkin, N.F., Ed., Moscow: Metallurgiya, 1980.

Translated by N. Korovin